$\delta = 168$ ($W_{1/2} = 800$ Hz); UV/Vis (*n*-pentane): λ_{max} 540 nm. **5**: m.p. (decomp) approximately 90 °C; ^{1}H NMR (250.133 MHz, C_6D_6, 300 K): $\delta = 0.25$ (CH_3), 8.04 (H_{arom}); ^{19}F NMR (235.36 MHz, C_6D_6, 300 K): $\delta = -66.6$ [*ortho*-CF_3, $J(^{207}Pb,^{19}F) = 374$ Hz, $^1J(^{19}F,^{13}C) = 275.4$ Hz]; -62.8 [*para*-CF_3, $^1J(^{19}F,^{13}C) = 272.5$ Hz]; UV/Vis (*n*-pentane): λ 586 nm; 1025 nm. Both compounds gave correct elemental analyses.

[5] Temperature-dependent ^{119}Sn NMR measurements, which would give valuable information about rearrangement processes or about the presence of a monomer/dimer equilibrium, could not be performed up to now for several reasons, such as very long aquisition times, the thermal lability of $\mathbf{4}_2$ at temperatures above room temperature, and the low solubility in inert solvents at low temperatures.

[6] G. Trinquier, *J. Am. Chem. Soc.* **1991**, *113*, 144.

[7] X-ray crystal structure analyses: P4 (Siemens), $\lambda(Mo_{K\alpha}) = 0.71073$ Å, ω scan mode, Lorenz and polarization correction, absorption correction (ψ scan, min/max. transmission: 0.73/0.99) for $\mathbf{5}_2$, solution by direct methods (SHELXS-86), refinement by a full-matrix least-squares procedure based on F_o^2 (SHELXL-93). $\mathbf{4}_2 \cdot C_5H_5$: monoclinic, space group $C2/c$ (no. 15), $a = 2213.3(4)$, $b = 1530.9(3)$, $c = 2057.1(4)$ pm, $\beta = 117.99(3)°$, $V = 6155(2)$ Å^3, $Z = 4$ (dimers), $\rho_{calcd} = 1.473$ Mgm^{-3}, $T = -100$ °C, $\mu = 1.049$ mm^{-1}, $3.4° < 2\theta < 55°$, 7264 measured reflections, 7080 independent, 332 parameters, 22 restraints, $R1$ [$F_o > 4\sigma(F_o)$] = 0.039, wR_2 [F_o^2; all data] = 0.110; $\mathbf{5}_2$: monoclinic, space group $I2/a$ (no. 15), $a = 2164.8(4)$, $b = 945.3(2)$, $c = 2864.2(6)$ pm, $\beta = 104.87(3)°$, $V = 5665(2)$ pm, $Z = 4$ (dimers), $\rho_{calcd} = 1.726$ Mgm^{-3}, $T = -100$ °C, $\mu = 6.190$ mm^{-1}, $3.9° < 2\theta < 48°$, 8675 measured reflections, 4419 independent, 289 parameters, $R1$ [$F_o > 4\sigma(F_o)$] = 0.038, wR_2 [F_o^2; all data] = 0.072. Crystallographic data (excluding structure factors) for the structures reported in this paper have been deposited with the Cambridge Crystallographic Data Centre as supplementary publication No. CCDC-100326. Copies of the data can be obtained free of charge on application to CCDC, 12 Union Road, Cambridge CB2 1EZ, UK (fax: int. code + (44) 1223 336033; e-mail: deposit@ccdc.cam.ac.uk).

[8] H. Jacobsen, T. Ziegler, *J. Am. Chem. Soc.* **1994**, *116*, 3667.

[9] Calculations: Equilibrium structures of E_2H_4 were determined by CCD (Sn) and CCSD (Pb) calculations (Gaussian 94) with Stuttgart quasi-relativistic pseudopotentials [W. Kuechle, M. Dolg, H. Stoll, H. Preuss, *J. Chem. Phys.* **1991**, *74*, 1245] and extended basis sets for Sn and Pb: (4s4p2d)/[5s5p2d]; basis sets for H: (3s2p)/[4s2p] [T. H. Dunning, *J. Chem. Phys.* **1970**, *19*, 553]. The dimerization energies were calculated at the CCSD level and have been corrected with respect to basis set superposition errors (full Counterpoise method) and zero-point vibrations. The identification of local minima on the hypersurface was verified by frequency calculations [NIMAG = 0].

[10] The definition of a double bond by means of quantum mechanics is based on the presence of two electron pairs shared by two nuclei. It is independent of the topology or the inherent bond energy. Thus—within the framework of LCAO-MO approximation (LCAO = *L*inear *C*ombination of *A*tomic *O*rbitals)—methods such as NBO (NBO = *N*atural *B*ond *O*rbitals) or NLMO analyses (NLMO = *N*aturally *L*ocalized *M*olecular *O*rbitals) can be used [J. E. Carpenter, F. Weinhold, *J. Mol. Struct. Theochem* **1988**, *169*, 41]. A further valuable method outside this framework is the Electron Localization Function (ELF), which is a function of the kinetic energy of the electrons [B. Silvi, A. Savin, *Nature* **1994**, *371*, 683]. We will present a detailed quantum chemical analysis of the bonding in compounds such as $\mathbf{5}_2$ using these methods elsewhere.

Dynamic Error Correction in Autocatalytic Peptide Networks**

Kay Severin, David H. Lee, Jose A. Martinez, Michael Vieth, and M. Reza Ghadiri*

Life operates precariously in between two extremes: evolution requires new information to be generated through mistakes during the self-reproduction step, but at the same time living systems need to preserve their information against excessive accumulation of errors.[1] Here we describe autocatalytic peptide networks that stabilize themselves against errors by subjugating the mutant population for the synthesis of the wild-type peptide. The systems are based on three or four peptide fragments that undergo competitive condensation reactions in neutral aqueous solutions to produce the native sequence of a peptide replicator along with its mutant products. The peptide self-replication process is shown to respond to the spontaneous formation of errors—experimentally simulated by the background coupling reactions that yield the mutant peptides—by employing the mutant product(s) as catalyst(s) for the synthesis of the native replicator sequence. Detailed analyses have revealed that this novel mode of sequence selection arises as the result of self-organization into networks composed of two or three interconnected (auto)catalytic cycles. These networks are among the first examples of biopolymer-based nonlinear chemical systems in which catalytic and autocatalytic processes are cooperatively coupled.[2]

The present study describes an unprecedented response of a self-replicating peptide system to the spontaneous generation of mutations by self-organizing into networks of cooperative autocatalytic and catalytic cycles that upregulates the production of the native sequence. The system is based on the recently reported sequence of a peptide replicator[3] and is composed of a maximum of four peptide fragments: the native electrophilic **E** and nucleophilic **N** fragments and their single alanine mutants $\mathbf{E_{9A}}$ and $\mathbf{N_{26A}}$, respectively (Figure 1). These peptides undergo competitive ligation reactions to produce four products: the native sequence **T** along with the single mutant peptides $\mathbf{T_{9A}}$ and $\mathbf{T_{26A}}$ and the double mutant peptide $\mathbf{T_{9/26A}}$. Thus addition of the mutant fragments to the initial mixture simulates the spontaneous formation of errors during the self-replication process. Furthermore, the mutations were chosen to be conservative replacements for the native amino acid residues (alanine in place of valine 9 or leucine 26) in order to simulate the production of a mutant population with a closely related informational content,[4] previously termed quasi-species.[5]

[*] Prof. Dr. M. R. Ghadiri, Dr. K. Severin, D. H. Lee
Dr. J. A. Martinez, Dr. M. Vieth
Departments of Chemistry and Molecular Biology, Skaggs Institute for Chemical Biology
The Scripps Research Institute
10550 North Torrey Pines Road, La Jolla, CA, 92037 (USA).
Fax: Int. code + (1) 619-784 2798
e-mail: ghadiri@scripps.edu

[**] We thank the Deutsche Forschungsgemeinschaft for a postdoctoral fellowship (K.S.), the Canadian Medical Research Council for a predoctoral fellowship (D.H.L.), and the Spanish Ministry of Education and Science for a postdoctoral fellowship (J.A.M.).

  1433-7851/98/3701-0126 $ 17.50+.50/0

E: ArCONH-RMKQLEEKVYELLSKVA-COSBn
E_{9A}: ArCONH-RMKQLEEK**A**YELLSKVA-COSBn
N: H_2N-CLEYEVARLKKLVGE-$CONH_2$
N_{26A}: H_2N-CLEYEVAR**A**KKLVGE-$CONH_2$
T: ArCONH-RMKQLEEKVYELLSKVACLEYEVARLKKLVGE-$CONH_2$
T_{9A}: ArCONH-RMKQLEEK**A**YELLSKVACLEYEVARLKKLVGE-$CONH_2$
T_{26A}: ArCONH-RMKQLEEKVYELLSKVACLEYEVAR**A**KKLVGE-$CONH_2$
$T_{9/26A}$: ArCONH-RMKQLEEK**A**YELLSKVACLEYEVAR**A**KKLVGE-$CONH_2$

$$E + N_{26A} + N \longrightarrow T + T_{26A} \quad (1)$$
$$E + E_{9A} + N \longrightarrow T + T_{9A} \quad (2)$$
$$E + E_{9A} + N + N_{26A} \longrightarrow T + T_{9A} + T_{26A} + T_{9/26A} \quad (3)$$
$$E + N_{26A} \xrightarrow{[T_{26A}]} T_{26A} \quad (4)$$
$$E_{9A} + N \xrightarrow{[T_{9A}]} T_{9A} \quad (5)$$
$$E + N_{26A} \xrightarrow{[T]} T_{26A} \quad (6)$$
$$E_{9A} + N \xrightarrow{[T]} T_{9A} \quad (7)$$
$$E + N \xrightarrow{[T_{9A}]} T \quad (8)$$
$$E + N \xrightarrow{[T_{26A}]} T \quad (9)$$
$$E + N \xrightarrow{[T_{9/26A}]} T \quad (10)$$

Figure 1. Fragment condensation reactions performed in this study and the corresponding peptide sequences. For the design principles, synthesis, characterization, and kinetic analyses, see ref. [3].

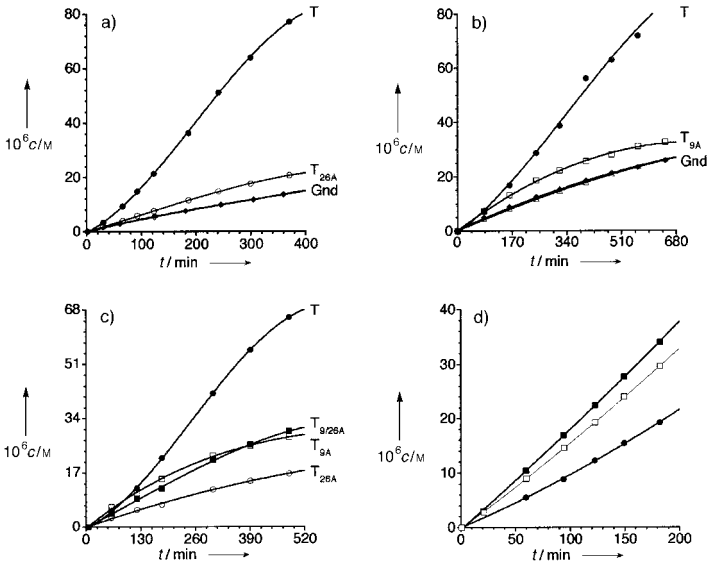

Figure 2. Product formation as a function of time. a) Reaction (1): **T** (●) and $\mathbf{T_{26A}}$ (○) and in the presence of 4 M Gnd **T** (◆) and $\mathbf{T_{26A}}$ (◇); b) reaction (2): **T** (●) and $\mathbf{T_{9A}}$ (□), and in the presence of 4 M Gnd **T** (◆) and $\mathbf{T_{9A}}$ (△); c) reaction (3): **T** (●), $\mathbf{T_{26A}}$ (○), $\mathbf{T_{9A}}$ (□), and $\mathbf{T_{9/26}}$ (■); d) reactions (8) and (9): **T** in the presence of 40 mM $\mathbf{T_{26A}}$ (□), 57 mM $\mathbf{T_{9A}}$ (■), or without any added template (●). It should be noted that the condensation of native fragments **N** and **E** is catalyzed by both single mutant products $\mathbf{T_{26A}}$ and $\mathbf{T_{9A}}$ [reactions (8) and (9) in d)], which leads to the pronounced selectivity for the native sequence **T** [reactions (1) – (3) in a) – c)].

Reaction mixtures composed of equimolar amounts of **E**, $\mathbf{N_{26A}}$, and **N** [Eq. (1)] or **E**, $\mathbf{E_{9A}}$, and **N** [Eq. (2)] in 4 M guanidinium (Gnd) solutions (pH 7.5) were shown to produce approximately equal amounts of the expected ligation products **T** and $\mathbf{T_{26A}}$ or **T** and $\mathbf{T_{9A}}$, respectively. This indicates a lack of kinetic preference for a specific ligation reaction under denaturing conditions. However, in the absence of denaturant, both reactions displayed pronounced preference for the production of the native peptide sequence **T** under neutral aqueous conditions (Figure 2a,b). A priori, the preferential production of the native peptide can be simply attributed to the known parabolic growth profile of the replicator sequence. Indeed, control experiments with equimolar amounts of **E** and $\mathbf{N_{26A}}$ [Eq. (4)] or $\mathbf{E_{9A}}$ and **N** [Eq. (5)] have shown that $\mathbf{T_{9A}}$ and $\mathbf{T_{26A}}$ are both incapable of catalyzing their own production. Therefore, the observed high selectivity in competitive ligation reactions can be attributed to a significant degree to the nonlinear growth profile of the peptide replicator[6] versus the linear background rate for the production of the mutants.

If one considers ternary complexes as the catalytically active intermediates,[3] for each reaction (1) and (2) there are two possible autocatalytic *and* two catalytic pathways that can lead to products formation (Figure 3). As suggested by the above experiments, pathways b and b′ for the autocatalytic production of the single mutant peptides $\mathbf{T_{9A}}$ and $\mathbf{T_{26A}}$ are not operative and the intermediate a is responsible for self-replication of the native sequence **T**. We therefore sought to examine the role of the remaining possible catalytic intermediates c, c′, d, and d′. Reactions composed of equimolar amounts of **E** and $\mathbf{N_{26A}}$ [Eq. (6)] or $\mathbf{E_{9A}}$ and **N** [Eq. (7)] do not

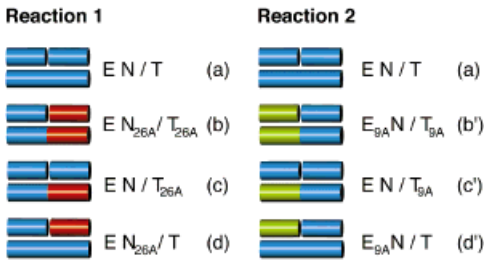

Figure 3. Schematic representation of plausible ternary intermediates for the autocatalytic (a, b, and b′) and catalytic (c, c′, d, and d′) production of ligation products in reactions (1) and (2). The ternary complexes are composed of an electrophilic peptide fragment (**E** or $\mathbf{E_{9A}}$), a nucleophilic peptide fragment (**N** or $\mathbf{N_{26A}}$), and the catalyst (**T**, $\mathbf{T_{9A}}$, or $\mathbf{T_{26A}}$). The different peptides are shown as colored cylinders to represent the α-helical configuration (native sequence: blue; E_{9A} and its corresponding T_{9A} segment: green; N_{26A} and its corresponding T_{26A} segment: red).

show any rate enhancements in the presence of added native peptide **T**. Therefore, the replicator sequence does not catalyze the formation of the mutant peptides, and pathways d and d′ are not operative. However, both single mutant peptides $\mathbf{T_{9A}}$ and $\mathbf{T_{26A}}$ catalyze the formation of the native sequence **T** [Eqs. (8) and (9), respectively; Figure 2d]. In fact, the catalytic efficiency of the mutant products for the production of the native sequence is approximately 75 % that of the native replicator sequence itself, as judged by the initial rate of product formation in the presence of similar amounts of added catalysts. The overall selectivity observed in reactions (1) and (2) is therefore the result of self-organized autocatlytic and catalytic cycles, which work in concert to favor the production of the native sequence **T** (Figure 4). It is

  1433-7851/98/3701-0127 $ 17.50+.50/0

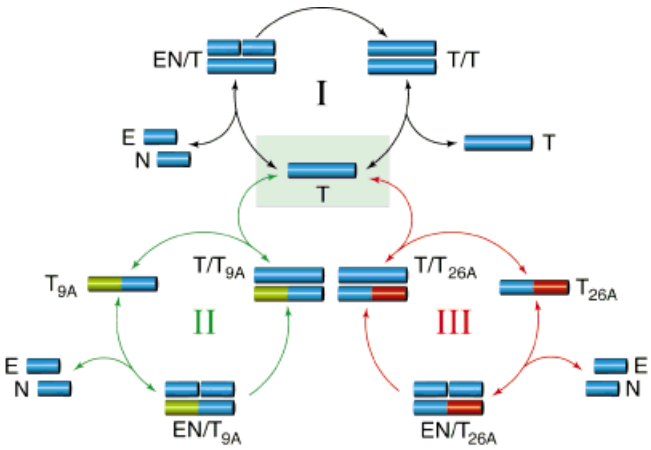

Figure 4. Peptide fragment condensations result in self-organized networks composed of two [cycles I and III or I and II for reactions (1) and (2), respectively] or three [reaction (3)] interconnected (auto)catalytic cycles with overall dynamic error-correcting properties. The mutant products $\mathbf{T_{9A}}$ (green-blue) and $\mathbf{T_{26A}}$ (red-blue) are infertile but catalyze the formation of the native replicator **T** (blue).

also interesting to note the asymmetry of the catalytic contribution: while the mutant peptides $\mathbf{T_{9A}}$ and $\mathbf{T_{26A}}$ are able to catalyze the formation of the native sequence **T**, **T** is "selfish" and does not accelerate the condensation of the mutant fragments. This unusual effect can be explained if one compares the stability of the intermediate ternary complex to the stability of the corresponding (self-inhibited) catalyst dimer. For reactions (6) and (7) the ternary complex is destabilized due to mutations in the hydrophobic core. Thus, the population of the intermediate is low, and no catalysis is observed. In Reactions (8) and (9), however, the mutation affects both the ternary complex and the catalyst dimer. The resulting increase in free catalyst concentration compensates for the reduced stability of the catalytic species.

The self-organized network persists also in reactions in which equimolar amounts of all four peptide fragments are employed [Eq. (3)]. In this case the double mutant product $\mathbf{T_{9/26A}}$ is not only infertile but also catalytically inactive [Eq. (10)]. Here the system is shown to self-organize into a network (*three* interconnected catalytic cycles), which displays a similar error-correction mechanism: each time a mutant product is formed, not only does it act as an efficient catalyst to generate several copies of the native sequence, but because these catalytic cycles are coupled to the native autocatalytic cycle, each new template produced in this way also serves to boost the production of the native sequence through the autocatalytic pathway (Figure 4). The net effect is significant upregulation in the production of the native peptide, leading to the selectivity observed in reactions (1)–(3) (Figure 2a–c).

The peptide-based systems described are the first examples of self-organized chemical networks that display characteristics essential for evolution: sequence-selective reproduction and dynamic error correction. Furthermore, these results suggest that short peptides are promising building blocks for complex nonlinear chemical systems, which may ultimately lead to the construction and understanding of molecular ecosystems.[7]

Experimental Section

All peptides were made by standard solid-phase peptide synthesis with *tert*-butyloxycarbonyl (Boc) chemistry. The electrophilic peptide fragments were synthesized as described previously.[3] The reactions were performed in 0.6 mL Eppendorf tubes. Temperature was maintained at 21.0($\pm$0.5)°C. A degassed, benzylthiol-saturated solution containing 3-(*N*-morpholino)-propane sulfonic acid (MOPS) buffer (pH 7.5), the nucleophilic peptide fragment(s) $\mathbf{N}_x$, and the internal standard 4-acetamidobenzoic acid (ABA) was incubated for 15 min. Reactions were initiated by adding a solution containing the electrophilic peptide fragment(s) $\mathbf{E}_y$ to give a total volume of 500 μL. Typically, the following final concentrations were employed: $\mathbf{N}_x = \mathbf{E}_y = 180-200\,\mu M$, MOPS = 140 μM, ABA = 100 μM. Peptide fragment condensations in the presence of Gnd ions (4 M) were performed as described above, except that MOPS buffer containing Gnd was used. Control experiments to probe (auto)catalytic contributions were performed with 15–40 mol% of the respective catalyst. All experiments were repeated twice. Samples (35 μL) were removed from the reaction vessel at various times, immediately quenched with 2% trifluoroacetic acid (70 μL), and stored at −78°C prior to HPLC analysis. Peptide concentrations were determined relative to the internal standard.

Received: June 6, 1997 [Z 10517 IE]
German version: *Angew. Chem.* **1998**, *110*, 133–135

Keywords: autocatalysis · error correction · networks · peptides · self-replication

[1] a) M. Eigen, P. Schuster, *Naturwissenschaften* **1971**, *58*, 465; b) B.-O. Küppers, *Information and the Origin of Life*, MIT Press, Cambridge, MA (USA) **1990**; c) S. A. Kauffman, *The Origins of Order*, Oxford Univ. Press, New York, **1993**.

[2] a) A hypercyclic peptide network that displays symbiosis among otherwise competitive peptide replicators: D. H. Lee, K. Severin, Y. Yokobayashi, M. R. Ghadiri, *Nature* **1997**, *390*, 591–594; b) nucleotide-based oligomers that display cross-catalytic behavior: D. Sievers, G. von Kiedrowski, *ibid.* **1994**, *369*, 221–224; c) synthetic structures that show cooperative behavior: J.-I. Hong, Q. Feng, V. Rotello, J. Rebek, Jr., *Science* **1992**, *255*, 848–850.

[3] a) D. H. Lee, J. R. Granja, J. A. Martinez, K. Severin, M. R. Ghadiri, *Nature* **1996**, *382*, 525–528; b) K. Severin, D. H. Lee, J. A. Martinez, M. R. Ghadiri, *Chem. Eur. J.* **1997**, 3, 1017–1024.

[4] Strong mutations such as placement of glutamic acid residues in the complementary hydrophobic interface have been shown previously to abolish template-directed catalysis.[3] Also see: J. C. Hu, E. K. O'Shea, P. S. Kim, R. T. Sauer, *Science* **1990**, *250*, 1400–1403.

[5] M. Eigen, P. Schuster, *The Hypercycle. A Principle of Natural Self-Organization*, Springer, Berlin, **1979**.

[6] A sigmoidal growth profile is a characteristic signature of efficient autocatalytic processes. This feature is clearly visible in reactions (1)–(3) (Figure 1).

[7] D. H. Lee, K. Severin, M. R. Ghadiri, *Curr. Opin. Chem. Biol.* **1997**, *1*, 491–496.

  1433-7851/98/3701-0128 $ 17.50+.50/0